Application of Machine Learning for Volumetric Analysis of Atherosclerotic Burden

Ana E. Cartaya [1,2,3,$], Sophie Maiocchi [2,3,4,5,$], Sarah Torzone[5], Geri Messinger[5], and Edward S. M. Bahnson[1,2,3,4,5]*

1. Dept. of Pharmacology
2. Center for Nanotechnology in Drug Delivery
3. McAllister Heart Institute
4. Curriculum of Toxicology and Environmental Medicine
5. Dept. of Cell Biology and Physiology
6. University of North Carolina at Chapel Hill, NC 27599, USA

$ These authors contributed equally

*To whom correspondence should be addressed:

Edward Moreira Bahnson, PhD.

Department of Cell Biology & Physiology

Center for Nanotechnology in Drug Delivery

115 Mason Farm Rd.

5109D Neuroscience Research Building (NRB) CB# 7545

University of North Carolina at Chapel Hill

Chapel Hill, NC 27599

Tel 919-843-0842

Email: edward_bahnson@med.unc.edu

ABSTRACT

Cardiovascular disease (CVD) remains the leading cause of mortality worldwide. Preclinical studies to research and validate therapeutic interventions for CVD often depend on two-dimensional histological surveys. The use of light sheet fluorescent microscopy together with optical clearing methods amenable to immunofluorescent staining are recent advances, all of which deliver detailed three-dimensional rendering of vessels. This offers the ability to describe and quantify features critical in CVD models, specifically, atherosclerotic plaque burden in atherosclerotic animal models. The main challenge for this approach remains the lengthy, hands-on, analysis time. Labkit is a user-friendly Fiji plugin that applies a machine-learning algorithm to create three-dimensional renderings from large microscopy data. The application of this plugin is expected to decrease the hands-on analysis time required to generate accurate volumetric renderings of atherosclerotic plaque burden in athero-prone mice. For analysis, Ldlr -/- (C57/Bl6) mice aged 6-8 weeks were fed a high-fat diet for 15 weeks to allow the development of atherosclerotic plaque along the aorta. Aged-matched chow-fed C57/Bl6 mice were used as athero-free controls. Aortic roots were sectioned and stained with hematoxylin and eosin, or oil red o stains, and later imaged and analyzed using ImageJ. AdipoClear and immunolabeling together with light-sheet fluorescent microscopy allowed for three-dimensional visualization. Both Imaris software v9.9.1 and the built-in bridge to ImageJ/Labkit were used to quantify the plaque burden in the mice manually or automatically, respectively. Our findings indicate that Labkit offers an effective and user-friendly platform for the segmentation of atherosclerotic plaque in aortas.

1. INTRODUCTION

Cardiovascular disease (CVD) persists as the leading cause of mortality in the world, with approximately one-third of deaths worldwide attributed to a cardiovascular event.[1,2] Atherosclerosis, a progressive inflammatory condition of the arteries, significantly contributes to CVD. The gradual subintimal deposition of proinflammatory lipoproteins and immune cells results in the development of atherosclerotic plaque in the affected arteries.[3] Thrombosis, a consequence of plaque rupture, can lead to serious clinical manifestations which include heart disease, stroke, and peripheral arterial disease.[3,4] Atherosclerosis is a highly complex, multifactorial disease, which is difficult to recapitulate with *in vitro* models.[5] As such, animal models are indispensable to understand the pathophysiology of atherosclerosis and discern effective therapeutic interventions.

Traditionally, methods to quantify atherosclerotic burden rely mainly on histological preparations of aortic root sections, and *en face* analysis of aortas. Both approaches are widely and frequently used, however, these methods lack universal standardization; and importantly fail to recapitulate the complex three-dimensional architecture of atherosclerotic plaque.[6,7] Recently, our lab and others validated the feasibility of coupling optical clearing methods amenable to immunofluorescent staining such as iDISCO+,[8,9] AdipoClear,[10] and CUBIC[11] with light sheet fluorescence microscopy (LSFM) for the three-dimensional (3D) rendering and analysis of medium to large-sized murine arteries. Further, our lab reported that LSFM processed arteries can be recovered, rehydrated, cryosectioned, and histologically processed with no significant effect on arterial size.[8] Also, we showed the feasibility of using the recovered arteries for additional immunofluorescent staining allowing for secondary multiplexing using the same samples. Altogether, LSFM appears the obvious choice for the 3D *ex vivo* analysis of vascular features in animal models of CVD. A major limitation for researchers looking to transition into

LSFM remains the arduous, time-consuming, manual segmentation required for the volumetric analysis of these large datasets.

In recent years, artificial intelligence (AI) methods have become more accessible across all disciplines.[12] The latest emergence of powerful microscopic imaging techniques allows for the visualization of biological structures in extraordinary detail, leaving scientists and physicians to decipher the best approach to extract relevant quantitative data from these datasets. To bridge the gap, several AI machine learning based automatic pixel classification and segmentation tools have been developed including CellProfiler,[13] Ilastik,[14] QuPath,[15] and Trainable Weka Segmentation[16]. Labkit,[17] the newest addition to this set of tools, is available as a Fiji plugin and unlike its predecessors, is capable of handling large 3D data without the need for specialized personal computers (PCs). Additionally, Labkit features a user-friendly interface with simple drawing tools hence making the application widely accessible to biomedical researchers. In this study, we aimed to validate this tool by comparing manual segmentation and Labkit's machine learning algorithm for the volumetric analysis of arteries. We show that Labkit derived pixel classification and automatic segmentation is an accurate and reliable method of analysis, henceforth widening the bottleneck in this data-rich approach. The overall aim of this article is then to further establish a methodology for analyzing common vascular features in animal models of CVD in a timely manner.

2. MATERIAL AND METHODS

2.1 Materials

Paraformaldehyde (PFA) (O4042-500; Thermo Fisher Scientific). Sodium azide (NaN_3) (S2002; Sigma-Aldrich). Sucrose (S0389; Sigma-Aldrich). Methanol (MX0475-1; Supelco). Phosphate buffered saline (PBS) (20-134; Apex Bioresearch Products). Glycine (A13816.0E; Thermo Fisher Scientific). Tween-20 (P1379; Sigma-Aldrich). Triton X-100 (X100; Sigma-Aldrich). Heparin sodium (H3393; Sigma-Aldrich). Dichloromethane (DCM) (650463; Sigma-Aldrich). Tris

base (BP152; Thermo Fisher Scientific). Acetic Acid (ARK2183; Sigma-Aldrich). Agarose (20-102GP; Apex Bioresearch Products). EDTA (BDH9232, VWR). Dibenzyl ether (DBE) (148400025; Thermo Fisher Scientific).

2.2 Animals

All animal protocols here described have been approved by the Institutional Animal Care and Use Committee (IACUC) of the University of North Carolina at Chapel Hill IACUC-ID (21-147). 6-7-week-old male $Ldlr^{-/-}$ mice (B6.129S7-Ldlrtm1Her/J, stock number: 002207), and C57Bl/6 mice (stock number: 000664) were obtained from The Jackson laboratory. Mice were allowed free access to food and water. After a week of acclimation, $Ldlr^{-/-}$ mice were started on a western high-fat diet consisting of 40% fat, 17% protein, 43% carbohydrate by kcal and 0.15% cholesterol by weight (RD Western Diet, catalog number: D12079Bi), while C57Bl/6 mice were fed standard chow for a total of 15 weeks. Mice were euthanized, and hearts and aortas were collected at 23 weeks.

2.3 Mouse aorta and aortic root collection

Aorta and hearts were collected following *in situ* perfusion-fixation with 10 mL of 1X PBS and 10 mL of 4% PFA in 1X PBS. To harvest the thoracic aorta, adipose tissue was carefully removed first, then the artery was cut at the aortic root and a few millimeters into the large three branches (brachiocephalic, left common carotid, and left subclavian arteries) while the aorta was excised at the bottom along the line of the diaphragm. Aortas and hearts were maintained in 4% PFA in 1X PBS at 4°C overnight, followed by two washes of PBS at room temperature the next day.

2.4 Mouse aorta immunostaining and processing for LSFM

Aortas were processed following the AdipoClear protocol,[18] with mild modifications. All steps were done at room temperature while shaking in 5 mL microtubes with 5 mL of liquid; except for

immunostaining, where samples are incubated in 1.7 mL microtubes with 1.5 mL of diluted antibody. Samples were dehydrated in an increasing methanol (MeOH) gradient (20%→40%→60%→80%→(2x)100%) v/v in B1n buffer (0.3M glycine, 0.1% Triton X-100, and 0.01% NaN_3 in dH_2O, pH 7) for 30 minutes per dilution. Samples were delipidated in three 100% dichloromethane (DCM) washes for 1 hour, overnight, and 1 hour the next day. Two washes of 100% MeOH were used to remove DCM, each 30 minutes. For immunostaining, aortas were rehydrated in a decreasing MeOH gradient (80%→60%→40%→20%) in B1n buffer, with two final washes in 100% B1n buffer for 30 minutes per dilution. The rehydrated samples were washed in PTxwH buffer (0.1% Triton X-100, 0.05% Tween 20, 0.01% NaN_3, and 2 µg/mL of heparin sulfate in 1X PBS) for 2 hours. Aortas were then probed with primary rabbit anti-mouse cd31 (50x, ab28364, Abcam) and rat anti-mouse cd68 (200x, MCA1957, Bio-Rad) diluted in PTxwH buffer for 4 days. Before, in between, and after secondary antibody probing, the samples were washed with PTxwH buffer 6 times for 30 minutes and a final time overnight. Aortas were probed sequentially using secondary donkey anti-rabbit IgG AF790 (200x, A11374, Thermo Fisher Scientific) and goat anti-rat PE (50x, STAR73, Bio-Rad) diluted in PTxwH buffer, each for 5 days. The nucleic acid stain TO-PRO™-3 Iodide (642/661) (5000x, T3605, Thermo Fisher Scientific) was added together with the final secondary antibody. Next, aortas were washed in PBS twice for 30 minutes, then warmed to 37°C for 1 hour and carefully embedded in 1% agarose (20-102GP; Apex Bioresearch Products) prepared in 1x TAE buffer. Once solidified, the agarose block containing the arteries was removed and dehydrated in an increasing MeOH gradient (20%→40%→60%→80%→(3x)100%) v/v in dH_2O for 30 minutes per dilution. The blocks were washed thrice with DCM for 1 hour, overnight, and 1 hour the next day. Arteries were cleared in glass scintillation vials using DBE overnight. Samples were stored in DBE in the dark until imaging.

2.5 LSFM acquisition

Imaging was done at the Microscopy Services Laboratory Core at UNC-Chapel Hill, in a LaVision BioTec Ultramicroscope II (Miltenyi Biotec, Germany) equipped with zoom body optics, an Andor Neo sCMOS camera (Andor Technology, United Kingdom), and an MVPLAPO 2X/0.5 objective (Olympus, Japan) fitted with a 5.7mm working distance corrected dipping cap allowing magnifications between 1.3-12.6X. Blocks were mounted in a resin sample holder and submerged into a container filled with DBE. Samples were imaged at 1.3X (0.63X zoom) and illuminated with a single sided, three light sheet configuration, with the waist of the sheet in the center of the aortic arch, an NA of 0.024 (beam waist at horizontal focus = 11.5 µm), and a light sheet width of 100% for even illumination in the y-axis. Images were acquired as two tiles with up to 40% overlap, and with a step size of 5 µm. Four channels were imaged as follows: tissue autofluorescence with a 488 nm laser excitation and a Chroma ET525/50m emission filter; CD68-PE with a 561 nm laser excitation and a Chroma ET600/50m emission filter; TO-PRO™-3 Iodide (642/661) with a 647 nm laser excitation and a Chroma ET690/50m emission filter; and CD31-AF790 with a 785 nm laser excitation and an ET800LP emission filter.

2.6 LSFM data processing

Files were exported as 16-bit ome.tif stacks and converted to Imaris (Bitplane, Oxford Instruments) .ims files with the Imaris File Converter software (v9.9.1). The Imaris tile files obtained were stitched with Imaris Stitcher (v9.9.1) with the final alignment done automatically or manually as needed. Imaris (v9.9.1) was used to visualize three dimensional projections with 3D viewer.

2.7 Manual segmentation

Manual plaque volume was determined using the manual drawing tools under the surface creation option in Imaris (v9.9.1) (Bitplane, Oxford Instruments). The plaque was delimited by cd31 staining in the lumen and diffuse autofluorescence around the border of the inner elastic

lamina. Contours were drawn along the anatomical axial and sagittal planes, ultimately rendering into a single surface with the unify option.

2.8 Labkit segmentation

Segmentation for plaque was done using the autofluorescence and endothelium (cd31) channels. Macrophage distribution in plaque was determined with a combination of the macrophage (cd68) and endothelium (cd31) channels. Labeling both foreground and background voxels was done with a brush size of 1. Default basic filters were used for analysis, as well as the option for GPU acceleration whenever available.

2.9 Aortic root histological processing, staining, and analysis

After perfusion-fixation and overnight 4% PFA incubation at 4°C as described above, hearts were bluntly cut at an angle parallel to the aortic sinus. The section containing the aortic root was transferred to 30% sucrose for overnight incubation at 4°C. Tissue was frozen in O.C.T. and stored at -80°C until processing. Frozen aortic roots were cut in 10 µm sections, 6 sections over 9 slides serially interrupted as recently recommended by the American Heart Association.[19] Matching slides per animal were stained with hematoxylin & eosin (H&E), or Oil red O (ORO). Sectioning and staining were done at Histology Research Core Facility at the University of North Carolina at Chapel Hill. Slides were imaged with the SLIDEVIEW VS200 (Olympus, Japan) at the Hooker Imaging Core at the University of North Carolina at Chapel Hill. Plaque, lumen, and necrotic core areas were measured using FIJI (https://imagej.net/software/fiji/).

2.10 Statistical analysis

Statistical analysis was conducted in Graphpad Prism version 9.3.1 (Graph Pad Software Inc., San Diego, CA). Analysis of any two groups was done using an unpaired Student's *t*-test. The best fit line between selected values was determined using a simple unconstrained linear regression, and the resulting R squared (r^2), p value and slope (m) reported.

3. RESULTS

The aim of this article is to validate Labkit, a user-friendly application of machine learning for automatic pixel classification and image segmentation, towards the accurate volumetric analysis of common vascular features gathered from LSFM processed arteries. The Labkit analysis workflow is illustrated in Figure 1, and it utilizes both Fiji and the integrated Labkit bridge to the Imaris software available on version 9.0 or higher.

3.1 Volumetric analysis of atherosclerotic plaque with machine learning based automatic pixel classification

Firstly, we once again validated the combination of LSFM and AdipoClear clearing protocol for the imaging of multiplexed immunostained thoracic aortas of high diet fed athero-prone mice, and age-matched chow fed C57/Bl6 mice. LSFM proves an outstanding approach to parse out anatomical details in these samples, as shown by the clear 3D projections in Figure 2A, and the original optical slices of aortic arch (Figure 2B) and descending aorta (Figure 2C) insets of the thoracic aortas processed. The optical slices, in particular, clearly show atherosclerotic plaque as the area delineated by the overlap of diffuse tissue autofluorescence (488 nm channel) and a bright cd31+ endothelium layer.

To determine the accuracy of Labkit's output to manual segmentation, aortas were manually labeled in Imaris using the contours function in the anatomical axial and sagittal planes. This was done because we found, on average, a 4-15% difference in the plaque volume obtained from doing only the axial plane when compared to both planes. Individual planes were transformed into surfaces that were then merged and unified resulting in the final manual segmentation volume. For Labkit segmentation the entire thoracic aorta was sparsely labeled, manually classifying a subset of pixels in three dimensions (voxels) as foreground, for areas of plaque, and background for everything else. After the initial training, the curation process, consisting of further labeling and training, was performed sporadically throughout the vessel,

supervising the algorithm for proper labeling. Once satisfied with the classifier, a one button operation takes care of automatically segmenting the entirety of the vessel in all dimensions resulting in the Labkit segmentation volume. It is crucial that the resulting Labkit volume be scrutinized for accuracy, as oftentimes edits need to be made prior to retrieving the final volume. Edits in Imaris are simple, using the available surface edit tools. In general, the resulting Labkit surface will include areas outside the arteries as it is the case that any remaining adventitial adipose tissue will have a similar texture as plaque and be recognized by the algorithm as such. Hence, it is important that excess adipose tissue be removed during the initial dissection of the vessel. The simplest method found to overcome this limitation is to save the trained classifier for batch processing within Imaris and generate smaller surfaces along the aorta excluding as much tissue outside the vessel as possible and lastly, merge all the resulting surfaces. Optical slices of the manual and Labkit segmentation, as well as their overlap, from a representative aortic arch (Figure 2B) and descending aorta (Figure 2C) illustrate the high accuracy of the automatic segmentation process performed by Labkit's machine learning algorithm. Detailed 3D reconstructions of the plaque generated manually or through Labkit, together with their resulting merged or overlapped surfaces (Figure 3A) also serve to illustrate this point. Volumetric results of plaque segmentation using the machine learning application reveal a strong linear relationship to manual segmentation (r^2=0.914, m=0.959, *$p < 0.05$) validating the reliability of the algorithm. Lastly, volumetric results obtained from Labkit significantly decrease hands-on analysis time by more than half the time taken to achieve the same manually.

3.2 Macrophage accumulation and distribution in atherosclerotic plaque

An additional major advantage provided by LSFM over traditional *en face* processing is the ability to stain the arteries for multiple targets. Macrophage accumulation and distribution in plaque is a common query among atherosclerosis researchers.[20] We sought then to determine if LSFM coupled with Labkit's analysis could feasibly provide a volumetric analysis of macrophage

distribution in cd31, and cd68+ aortas. Optical sections (Figure 4A) and 3D reconstructions (Figure 4B) of the macrophage (cd68+) layer shows extensive distribution of macrophages throughout the volume of atherosclerotic plaque. We found that plaque and macrophage volumes show a strong positive linear relationship (r^2=0.974, m=0.280, *$p < 0.05$) (Figure 4C) increasing with plaque volume.

4. DISCUSSION

Herein, we describe the application of a machine learning tool, Labkit, for the quantitative analysis of atherosclerotic plaque burden in the aortas of atherosclerotic-prone mice. Firstly, we demonstrated that the Labkit derived plaque volume is significantly correlated with the volume resulting from manual analysis, confirming the accuracy and reliability of Labkit for volumetric analysis of atherosclerotic plaque. Importantly, the implementation of our protocol results in a significant reduction in the time required to analyze plaque volumes, (on average 4 hrs to less than 1 hr), with this including short periods of hands-off training. Secondly, we show that the Labkit obtained plaque volumes, together with the modest volumes of plaque developed by the control C57/Bl6 mice positively and strongly correlate to the average aortic lesion area in the aortic root, determined by traditional histological methods in agreement with established results.[21] This further confirms the reliability of Labkit derived plaque volume measurements. Finally, we demonstrate that this protocol can be multiplexed for analysis of other plaque characteristics such as inflammatory cell distribution. Overall, we present a method that significantly reduces the time to analyze plaque volumes from 3D LSFM datasets. This method does not require neither specialized PCs nor specialized computational skills, and is therefore a step toward making LSFM more widely adopted as an accurate volumetric quantitation technique.

Atherosclerosis is a complicated disease, with numerous factors contributing to its development. Unsurprisingly, even the latest established *in vitro* models fail to fully recapitulate the disease.[5]

As such, preclinical animal models, such as the Ldlr$^{-/-}$ and ApoE$^{-/-}$ mice, are essential in aiding our understanding of atherosclerotic disease initiation and progression. Both atherosclerotic plaque burden and volume are two key characteristics that are utilized as a measure of either the influence of a genetic mutation or of a therapeutic intervention upon disease. Current widely-used techniques to analyze plaque volume and burden in atherosclerotic mice rely either on histological sectioning of the aortic sinus[22,23] as developed originally by Paigen and co-workers in 1987[24], or *en face* staining of the aorta with lipid staining dyes such as Sudan IV or Oil red O.[25] Both techniques have significant drawbacks including the introduction of several sources of variability that decrease the accuracy of plaque burden measurements, thereby increasing the variability of an already highly variable disease model.

More recently, advanced 3D imaging techniques have come to the forefront to describe and quantitate atherosclerotic plaque volume in preclinical models, including high resolution magnetic resonance imaging (MRI),[26] microscopic computed tomography (microCT),[27] and optical projection tomography (OCT).[28] In line with this growing focus on 3D imaging techniques, us and others have demonstrated the utility of LSFM together with clearing protocols amenable to immunofluorescent staining, such as AdipoClear[10] and iDISCO+[8], to provide 3D unbiased quantitative measurements of vascular injury.[8-10] Additionally, previous research has demonstrated that there is a significant correlation between plaque burden obtained by *en face* staining, and volume obtained through microCT imaging;[29] which indicates that 3D techniques could replace *en face* staining as these approaches become increasingly available, user-friendly and lower cost. Thus far, the major limitation of using LSFM for the quantification of plaque burden is the large investment on the hand-on analysis time, which limits its application to typically large datasets seen in preclinical studies. The methodology described herein is a step towards reliable quantitation of 3D datasets using an accessible machine learning application with a significantly lower hands-on analysis time.

Previous authors have applied artificial intelligence approaches in both the clinical,[30-32] and preclinical settings to detect, quantify and classify atherosclerotic plaque. Jurtz and co-authors recently detailed a deep learning model that was trained for plaque quantification in different anatomical segments of the mouse aorta.[9] This method resulted in reliable and accurate measurements of plaque volume. However, the major limitations of this approach are often the need for expensive, powerful computers and skills from researchers, as well as the need for large training datasets. The field does continue to take incremental steps toward making deep learning models more accessible, and cost-effective.[33] An alternative machine learning algorithm, random forests, requires much less training data. As such several tools have been developed for the imaging community, all unable to process large image data. Labkit, also an application of the random forests algorithm, fills that gap.[17] The application features a simple layout for pixel classification and is easily accessed through Fiji to quickly segment large image data. It also features a dedicated documentation page in the ImageJ Wiki (https://imagej.net/plugins/labkit/). Altogether, highlighting the utility of Labkit for the quantitative analysis of atherosclerotic plaque.

In addition to atherosclerotic plaque volume and burden, other aspects of atherosclerosis are of relevance. The inflammatory characteristics, including inflammatory cell distribution, as well as necrotic core size, and endothelial erosion are all of interest to quantify. LSFM allows us to multiplex with different molecular markers. Herein we have shown the presence of cd31 as well as cd68 to probe some of the mentioned characteristics. In particular, we show that macrophage content is highly correlated with plaque volume, an effect previously reported in human atherosclerotic arterial samples.[34] Lastly, distribution of macrophages appears restricted to the periphery of larger plaques that develop in the aortic arch, in contrast to the smaller plaque that develops in the descending aorta which appear more thoroughly infiltrated by the

inflammatory cells. Similar observations were made by Jurtz et al, with subtle differences in distribution of cd45 signal.[9]

Important limitations remain for the use of LSFM and Labkit volumetric analysis of atherosclerotic plaque. Firstly, current commercially available LSFM equipment, in general, achieves modest cellular resolution compared to well-established techniques like laser scanning confocal microscopy. LSFM techniques continue to improve at an accelerated rate, with researchers looking to answer questions in subcellular resolution. Recent research suggests that the technology to answer these questions is around the corner, for example, the combination of LSFM and the super resolution technique, structured illumination microscopy (SIM), pushes the lateral resolution to less than 100 nm.[35,36] Another limitation to the broad adoption of LSFM is the necessary optical clearing step, and validation of compatible antibodies for immunostaining, both of which remain a large time investment.[37] Additionally, with regards to the Labkit analysis, the application segmentation algorithm classifies pixels independent of their position in the image.[17] In the case where significant adventitial fat is still present, for example, Labkit may include this tissue in the final plaque volume. As such, it is crucial that the resulting volume be edited for accurate plaque representation, which can add up to an hour to the process. It is possible to overcome this limitation by processing the samples in smaller sections, ultimately merging all resulting surfaces.

In conclusion, we describe and validate the application of a user-friendly machine learning algorithm for automatic 3D segmentation, Labkit, to provide accurate volumetric quantitation of atherosclerotic plaque from murine preclinical models of arteriosclerotic vascular disease. Overall, the protocol presented reduces the plaque volume quantitation time to less than an hour. Our technique also allows for the simultaneous analysis of other important plaque features, such as inflammatory cell content by staining for macrophage markers. This greatly increases the practicality of LSFM for the analysis of large data sets of mice, which are typical in

studies of atherosclerosis, where the variability typically necessitates 10-15 mice per treatment group. Moreover, this algorithm is a widely available Fiji plugin, with no need for specialized PCs, computational skills, or access to large training data sets necessary for deep learning. Thus, literature reports of this application are expected to increase both the appeal of LSFM and these analysis techniques. It is likely this protocol can be successfully applied to other vascular tissue in preclinical vascular disease animal models, including the aortic root. Finally, if need be, in our previous studies we have shown that vascular tissue samples can be recovered, rehydrated, embedded in O.C.T, and sectioned, following LSFM imaging.[8]

5. FIGURES

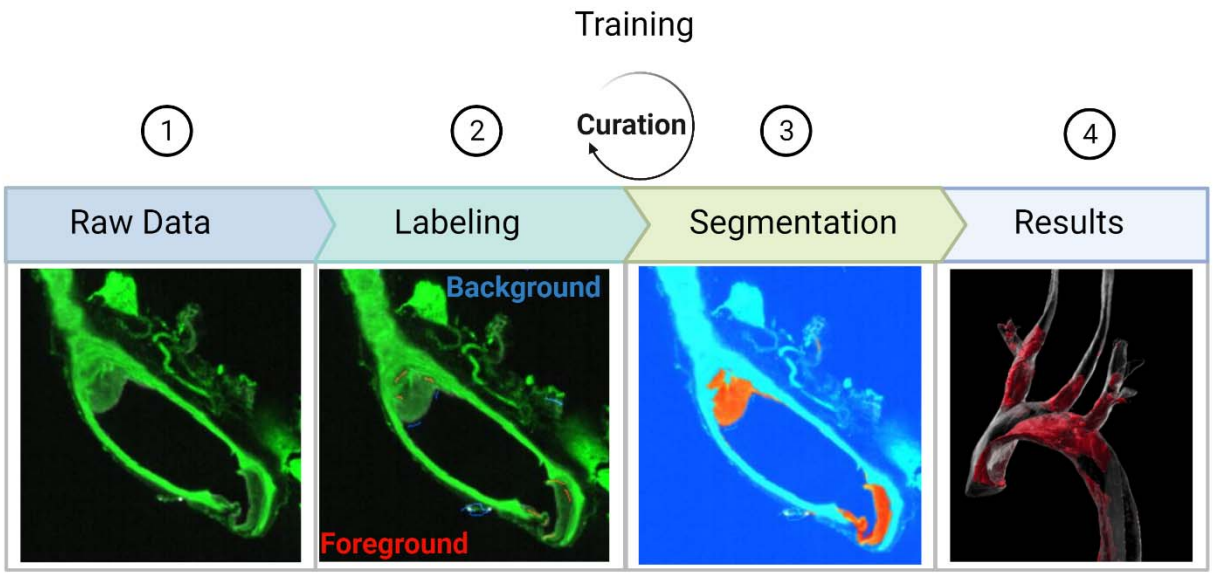

Figure 1. Overview of the Labkit image segmentation process. Step 1. LSFM was used to image the thoracic aortas of athero-prone mice. Step 2. Scribble labeling for binary classification of the plaque (foreground) and not plaque (background) results in automatic segmentation along the artery shown in the next step. Step 3. Orange labeling indicates plaque volume, whilst blue labeling indicates tissue that is not plaque as determined by the algorithm after training. Step 4. Labkit automatically segments the plaque volume in the 3D space of the entire aorta. The final result is the automatic production of a plaque volume surface, labeled here in red.

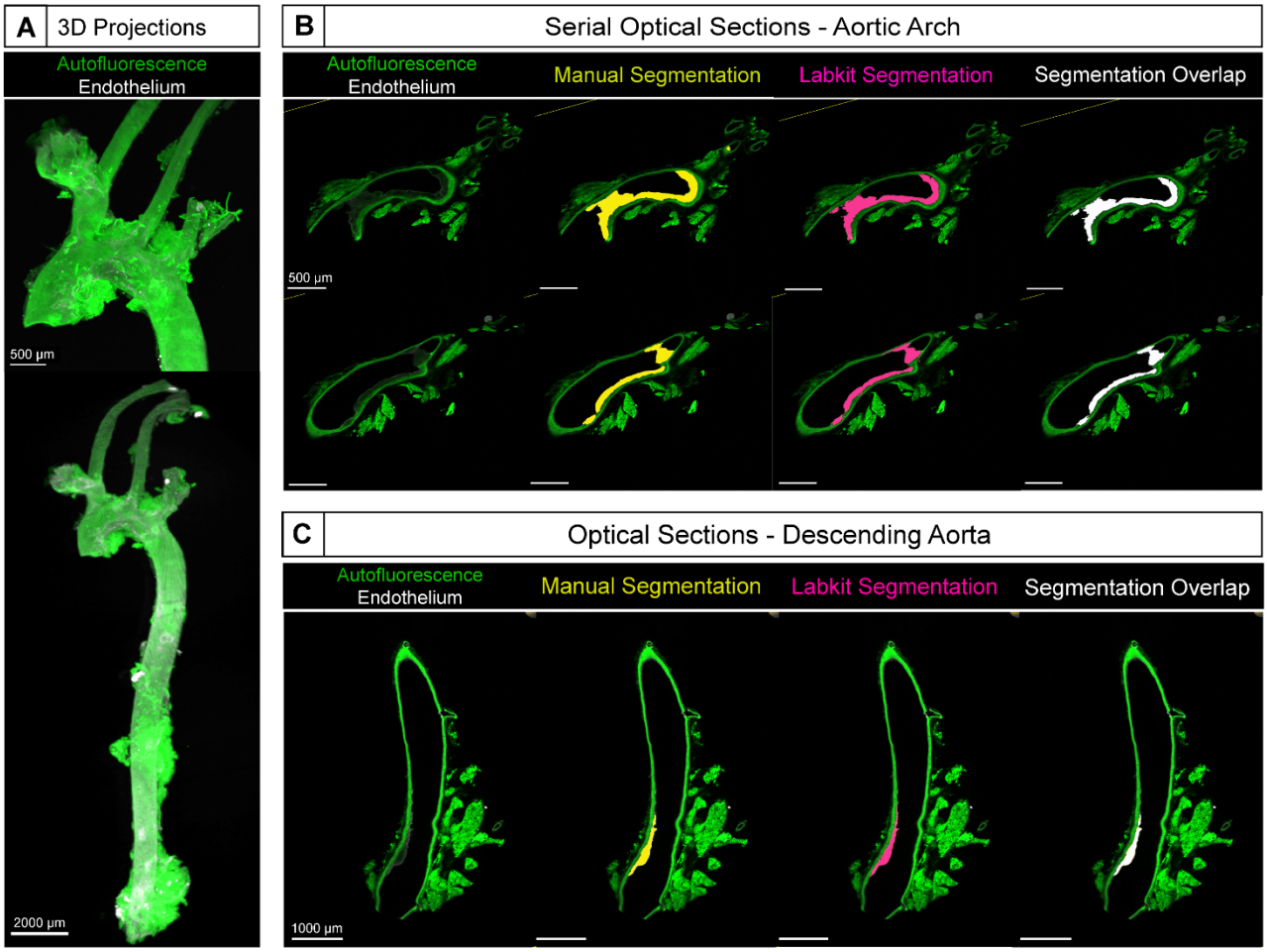

Figure 2. Light sheet fluorescent microscopy coupled with Labkit derived segmentation results in accurate pixel classification of atherosclerotic plaque. (A) 3D volume of a representative mouse aortic arch (top, scale bar = 500 µm) and complete thoracic aorta (bottom, scale bar = 2000 µm) obtained using light sheet fluorescent microscopy. Optical sections representatives from a single aorta (B) aortic arch, and (C) descending aorta showing atherosclerotic plaque delineated by both tissue autofluorescence and the endothelium marker cd31, together with manual, or Labkit based segmentation and their overlap. Scale bar = 500 µm (B), 1000 µm (C).

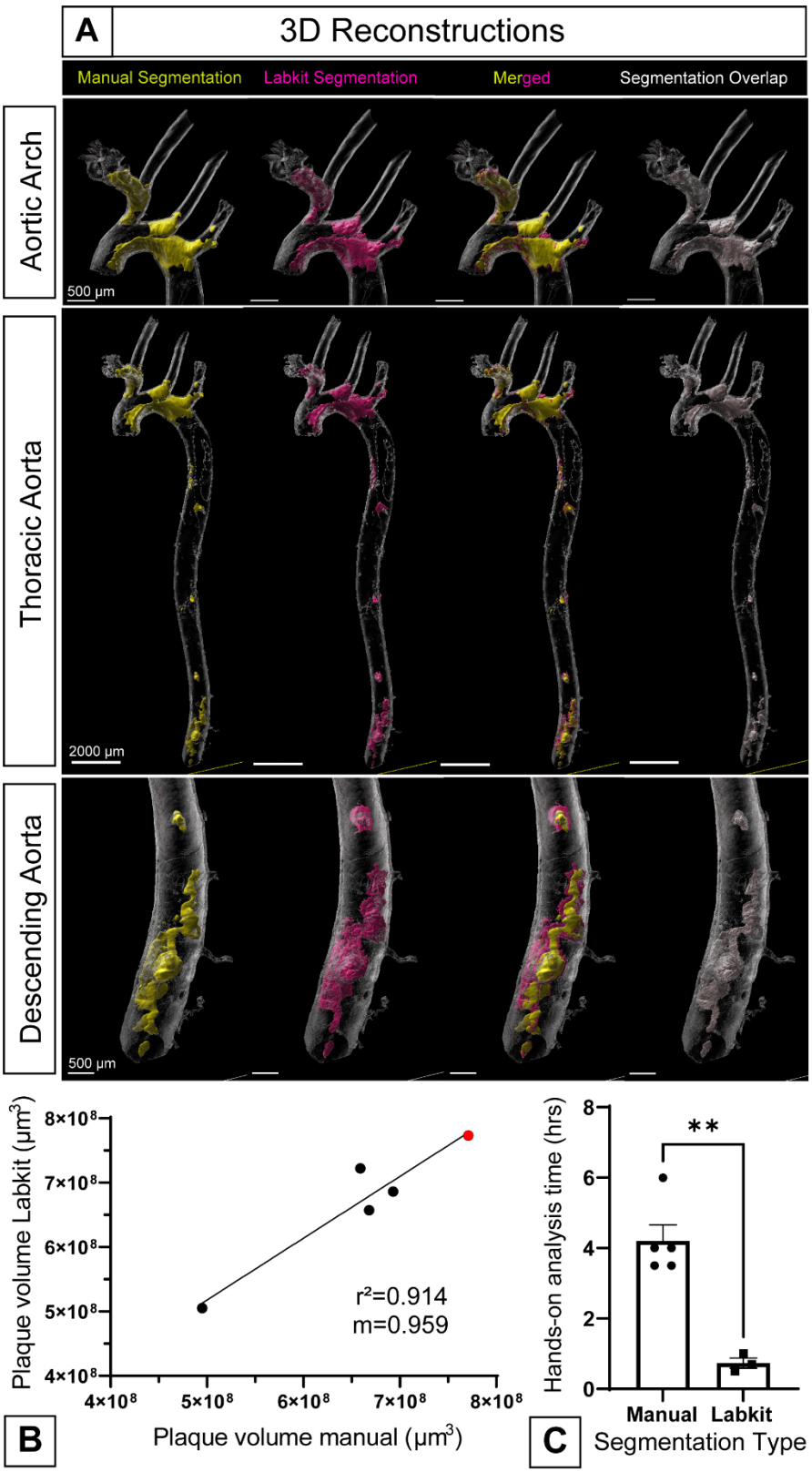

Figure 3. Labkit based volumetric analysis results in accurate labeling of atherosclerotic plaque with a significantly shortened hands-on analysis time. (A) 3D reconstructions of manual, and Labkit based segmentation of atherosclerotic plaque in a representative mouse thoracic aorta (middle, scale bar = 2000 µm) with a zoomed view into atherosclerotic plaque rich areas of the aortic arch (top) and the descending aorta (bottom); top and bottom scale bars = 500 µm. (B) Best fit line of the linear regression between manual and Labkit derived segmentation (n=5, r^2=0.914, m=0.959, *p < 0.05) Representative aorta from (A) shown in red (C) Hands-on analysis time taken for manual segmentation compared to Labkit (means ± SEM, n=5, **p < 0.01).

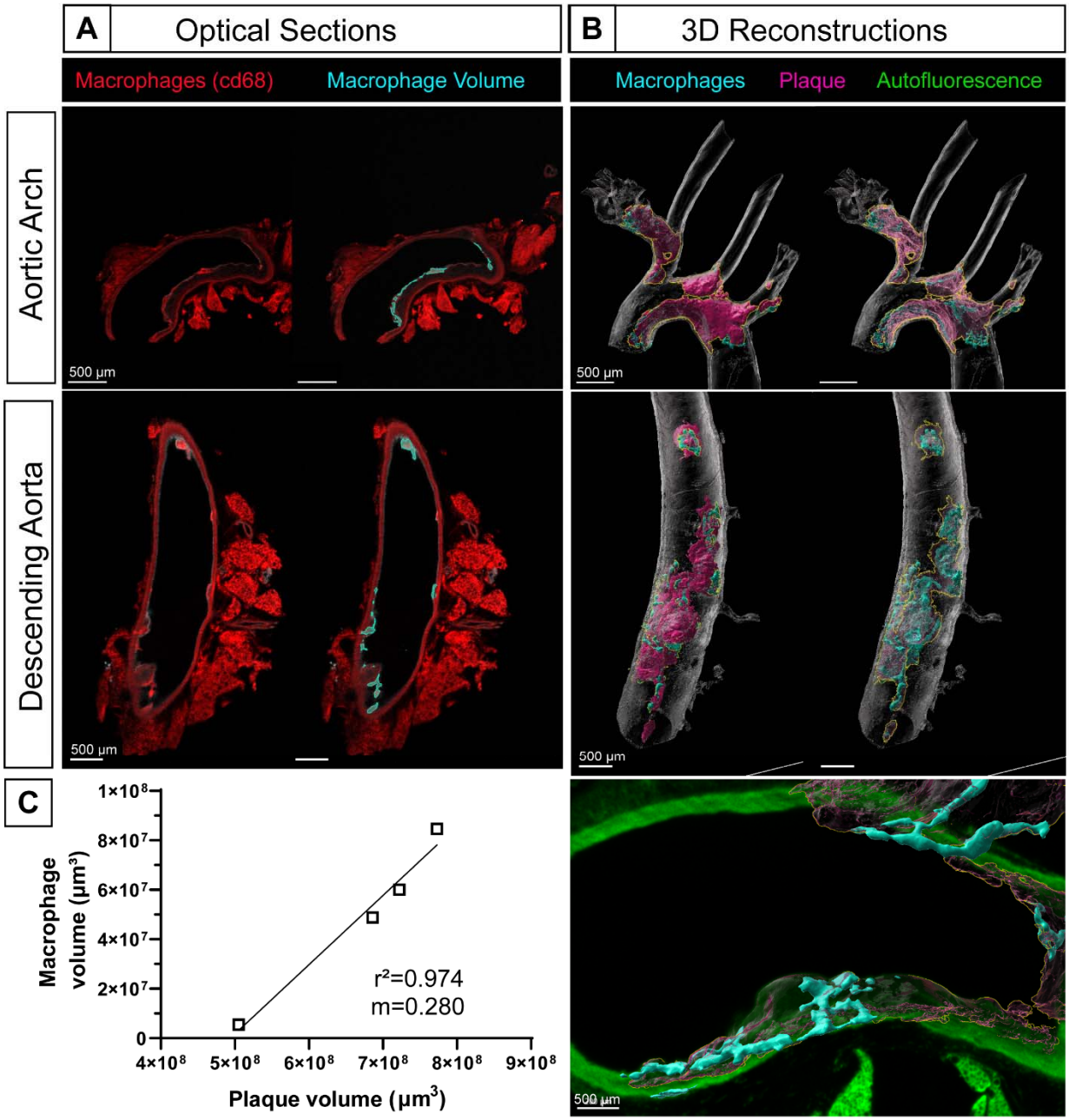

Figure 4. Labkit-enabled volumetric analysis of plaque-associated macrophages reveals a linear relationship with plaque volume. (A) Representative optical sections from a single aorta (top) aortic arch, and (bottom) descending aorta displaying macrophage infiltration in atherosclerotic plaque delineated by the endothelium marker cd31 and macrophage marker cd68, compared to the same optical section with the resulting Labkit segmentation slice. Scale bar = 500 µm (B) 3D reconstructions of a representative mouse thoracic aorta with Labkit derived plaque and macrophage volumes in (top) aortic arch, and (bottom) descending aorta

showing plaque as a solid or transparent surface. (Bottom) Zoomed in optical section of the aortic arch with high plaque burden, together with 3D reconstructions of atherosclerotic plaque and macrophage volumes. Scale bar = 500 µm. (C) Best fit line of the linear regression between Labkit derived plaque and macrophage volumes (n=4, r^2=0.974, m=0.280, *p < 0.05).

SUPPLEMENTAL

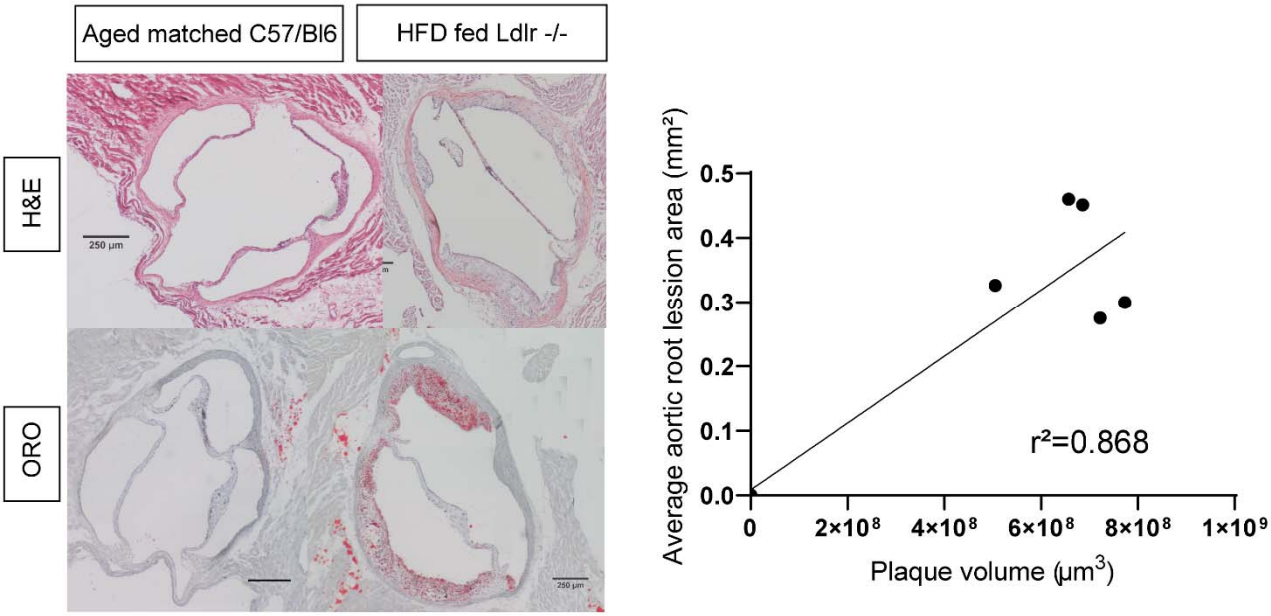

Supplemental Figure 1. Correlation between plaque volume in the aortic arch and the average lesion area in the aortic root of the same animals. Representative histological sections of H&E and Oil Red O stained aortic roots of age-matched C57/Bl6 control mice chow fed, or high fat diet fed $Ldlr^{-/-}$ mice. Best fit line of the linear regression between plaque volume and average aortic root lesion area (n=5 for both groups, r^2=0.868, ****p < 0.001).

CONFLICTS OF INTEREST

The authors declare no conflicts of interest regarding the publication of this manuscript.

ACKNOWLEDGMENTS

This work was supported by the National Institutes of Health, National Heart Lung, and Blood Institute [K01HL145354]. A.E.C is supported by the National Heart, Lung, and Blood Institute Predoctoral Fellowship [F31HL156427]. S.M is supported by supported by the National Heart, Lung, and Blood Institute Pathway to Independence Award (K99/R00) [K99HL157690]. LSFM imaging was done at the UNC Microscopy Services Laboratory Core supported, in part, by the P30 CA016086 Cancer Center Core Support Grant to the UNC Lineberger Comprehensive Cancer Center, and the North Carolina Biotech Center Institutional Support Grant 2016-IDG-1016. Slide imaging was performed at UNC Hooker Imaging Core Facility, supported in part by P30 CA016086 Cancer Center Core Support Grant. Sectioning and histological processing were done at Histology Research Core Facility at the University of North Carolina at Chapel Hill.

REFERENCES

1 Tsao, C. W. *et al.* Heart Disease and Stroke Statistics-2022 Update: A Report From the American Heart Association. *Circulation* **145**, e153-e639, doi:10.1161/CIR.0000000000001052 (2022).

2 Organization, G. W. H. (2022).

3 Milutinovic, A., Suput, D. & Zorc-Pleskovic, R. Pathogenesis of atherosclerosis in the tunica intima, media, and adventitia of coronary arteries: An updated review. *Bosn J Basic Med Sci* **20**, 21-30, doi:10.17305/bjbms.2019.4320 (2020).

4 Bergheanu, S. C., Bodde, M. C. & Jukema, J. W. Pathophysiology and treatment of atherosclerosis : Current view and future perspective on lipoprotein modification treatment. *Neth Heart J* **25**, 231-242, doi:10.1007/s12471-017-0959-2 (2017).

5 Chen, J. *et al.* Recent Progress in in vitro Models for Atherosclerosis Studies. *Front Cardiovasc Med* **8**, 790529, doi:10.3389/fcvm.2021.790529 (2021).

6 Chen, H. *et al.* A mini-review on quantification of atherosclerosis in hypercholesterolemic mice. *Glob Transl Med* **1**, doi:10.36922/gtm.v1i1.76 (2022).

7 Lin, Y. *et al.* Practical assessment of the quantification of atherosclerotic lesions in apoE(-)/(-) mice. *Mol Med Rep* **12**, 5298-5306, doi:10.3892/mmr.2015.4084 (2015).

8 Buglak, N. E. *et al.* Light sheet fluorescence microscopy as a new method for unbiased three-dimensional analysis of vascular injury. *Cardiovasc Res* **117**, 520-532, doi:10.1093/cvr/cvaa037 (2021).

9 Jurtz, V. I. *et al.* Deep learning reveals 3D atherosclerotic plaque distribution and composition. *Sci Rep* **10**, 21523, doi:10.1038/s41598-020-78632-4 (2020).
10 Becher, T. *et al.* Three-Dimensional Imaging Provides Detailed Atherosclerotic Plaque Morphology and Reveals Angiogenesis After Carotid Artery Ligation. *Circ Res* **126**, 619-632, doi:10.1161/circresaha.119.315804 (2020).
11 Souilhol, C. *et al.* JAG1-NOTCH4 mechanosensing drives atherosclerosis. *Sci Adv* **8**, eabo7958, doi:10.1126/sciadv.abo7958 (2022).
12 Krenn, M. *et al.* On scientific understanding with artificial intelligence. *Nat Rev Phys* **4**, 761-769, doi:10.1038/s42254-022-00518-3 (2022).
13 McQuin, C. *et al.* CellProfiler 3.0: Next-generation image processing for biology. *PLoS Biol* **16**, e2005970, doi:10.1371/journal.pbio.2005970 (2018).
14 Berg, S. *et al.* ilastik: interactive machine learning for (bio)image analysis. *Nat Methods* **16**, 1226-1232, doi:10.1038/s41592-019-0582-9 (2019).
15 Bankhead, P. *et al.* QuPath: Open source software for digital pathology image analysis. *Sci Rep* **7**, 16878, doi:10.1038/s41598-017-17204-5 (2017).
16 Arganda-Carreras, I. *et al.* Trainable Weka Segmentation: a machine learning tool for microscopy pixel classification. *Bioinformatics* **33**, 2424-2426, doi:10.1093/bioinformatics/btx180 (2017).
17 Arzt, M. *et al.* LABKIT: Labeling and Segmentation Toolkit for Big Image Data. *Frontiers in Computer Science* **4**, doi:10.3389/fcomp.2022.777728 (2022).
18 Chi, J., Crane, A., Wu, Z. & Cohen, P. Adipo-Clear: A Tissue Clearing Method for Three-Dimensional Imaging of Adipose Tissue. *J Vis Exp*, doi:10.3791/58271 (2018).
19 Daugherty, A. *et al.* Recommendation on Design, Execution, and Reporting of Animal Atherosclerosis Studies: A Scientific Statement From the American Heart Association. *Arterioscler Thromb Vasc Biol* **37**, e131-e157, doi:10.1161/ATV.0000000000000062 (2017).
20 Makhani, K. *et al.* Using the Apolipoprotein E Knock-Out Mouse Model to Define Atherosclerotic Plaque Changes Induced by Low Dose Arsenic. *Toxicol Sci* **166**, 213-218, doi:10.1093/toxsci/kfy201 (2018).
21 Tangirala, R. K., Rubin, E. M. & Palinski, W. Quantitation of atherosclerosis in murine models: correlation between lesions in the aortic origin and in the entire aorta, and differences in the extent of lesions between sexes in LDL receptor-deficient and apolipoprotein E-deficient mice. *J Lipid Res* **36**, 2320-2328 (1995).
22 Baglione, J. & Smith, J. D. Quantitative assay for mouse atherosclerosis in the aortic root. *Methods Mol Med* **129**, 83-95, doi:10.1385/1-59745-213-0:83 (2006).
23 Venegas-Pino, D. E., Banko, N., Khan, M. I., Shi, Y. & Werstuck, G. H. Quantitative analysis and characterization of atherosclerotic lesions in the murine aortic sinus. *J Vis Exp*, 50933, doi:10.3791/50933 (2013).
24 Paigen, B., Morrow, A., Holmes, P. A., Mitchell, D. & Williams, R. A. Quantitative assessment of atherosclerotic lesions in mice. *Atherosclerosis* **68**, 231-240, doi:10.1016/0021-9150(87)90202-4 (1987).
25 Centa, M., Ketelhuth, D. F. J., Malin, S. & Gisterå, A. Quantification of Atherosclerosis in Mice. *J Vis Exp*, doi:10.3791/59828 (2019).
26 McAteer, M. A. *et al.* Quantification and 3D reconstruction of atherosclerotic plaque components in apolipoprotein E knockout mice using ex vivo high-resolution MRI. *Arterioscler Thromb Vasc Biol* **24**, 2384-2390, doi:10.1161/01.ATV.0000146811.19029.fb (2004).
27 Martinez, H. G. *et al.* Images in cardiovascular medicine: Microscopic computed tomography-based virtual histology for visualization and morphometry of atherosclerosis in diabetic apolipoprotein e mutant mice. *Circulation* **120**, 821-822, doi:10.1161/circulationaha.108.829531 (2009).

28 Kirkby, N. S. *et al.* Quantitative 3-dimensional imaging of murine neointimal and atherosclerotic lesions by optical projection tomography. *PLoS One* **6**, e16906, doi:10.1371/journal.pone.0016906 (2011).
29 Lloyd, D. J. *et al.* A volumetric method for quantifying atherosclerosis in mice by using microCT: comparison to en face. *PLoS One* **6**, e18800, doi:10.1371/journal.pone.0018800 (2011).
30 Munger, E. *et al.* Application of machine learning in understanding atherosclerosis: Emerging insights. *APL Bioeng* **5**, 011505, doi:10.1063/5.0028986 (2021).
31 Zhang, J., Han, R., Shao, G., Lv, B. & Sun, K. Artificial Intelligence in Cardiovascular Atherosclerosis Imaging. *J Pers Med* **12**, doi:10.3390/jpm12030420 (2022).
32 Lu, H. *et al.* Research Progress of Machine Learning and Deep Learning in Intelligent Diagnosis of the Coronary Atherosclerotic Heart Disease. *Comput Math Methods Med* **2022**, 3016532, doi:10.1155/2022/3016532 (2022).
33 von Chamier, L. *et al.* Democratising deep learning for microscopy with ZeroCostDL4Mic. *Nat Commun* **12**, 2276, doi:10.1038/s41467-021-22518-0 (2021).
34 Tearney, G. J. *et al.* Quantification of macrophage content in atherosclerotic plaques by optical coherence tomography. *Circulation* **107**, 113-119, doi:10.1161/01.cir.0000044384.41037.43 (2003).
35 Chang, B. J., Perez Meza, V. D. & Stelzer, E. H. K. csiLSFM combines light-sheet fluorescence microscopy and coherent structured illumination for a lateral resolution below 100 nm. *Proc Natl Acad Sci U S A* **114**, 4869-4874, doi:10.1073/pnas.1609278114 (2017).
36 Chen, B. *et al.* Resolution doubling in light-sheet microscopy via oblique plane structured illumination. *Nat Methods* **19**, 1419-1426, doi:10.1038/s41592-022-01635-8 (2022).
37 Delgado-Rodriguez, P., Brooks, C. J., Vaquero, J. J. & Munoz-Barrutia, A. Innovations in ex vivo Light Sheet Fluorescence Microscopy. *Prog Biophys Mol Biol* **168**, 37-51, doi:10.1016/j.pbiomolbio.2021.07.002 (2022).